Supplementary information:

Double Layer Capacitance of Anode/Solid-electrolyte Interfaces

Xiaoming Ge[a,b],* *Changjing Fu*[a,b], *Siew Hwa Chan*[a,b] *

a. School of Mechanical and Aerospace Engineering, Nanyang Technological University, Singapore, 639798. Email: ge0001ng@e.ntu.edu.sg ; MSHCHAN@ntu.edu.sg

b. Energy Research Institute at NTU (ERI@N), Singapore, 637553.

Appendix A: Gouy−Chapman Capacitance of the LSV/YSZ interfaces

The Volta potential difference of the Gouy−Chapman (G–C) layer is divided into two parts: one is the linear part starting from the electrode/electrolyte interface to outer Helmholtz plane (oHp), and the other is the non-linear part decaying asymptotically into bulk electrolyte (Fig. 3a). While the linear part is described by the double-plate condenser model, the non-linear part calls for a Debye and Hückel's treatment. Main assumptions in this study are: (*i*) charge cloud approximation. Some oxygen vacancies are immobilized on the outer Helmholtz plane (oHp). The others beyond the oHp are smeared into continuous thermal disarray, thus creating a charge cloud from oHp to the bulk YSZ; (*ii*) continuum. The bulk YSZ is treated as a continuous dielectric medium; (*iii*) one dimension. The charge distribution is uniform in directions parallel to the LSV/YSZ interface; (*iv*) time-invariant. All treatments are in steady state conditions. Transient states with electric-magnetic interactions are not taken into account; (*v*) negligible electron and hole effects. Electron and hole concentrations are in orders lower than that of oxygen vacancies in the bulk YSZ. The electroneutrality is maintained by Y'_{Zr} and $V_O^{\cdot\cdot}$.

For the sake of mechanistic lucidity we start from the derivation of Poisson's equation. Consider a Gaussian pillbox with radius r and length l (Fig. 3a).[1] One of its two lateral surfaces situates in the LSV side and the other locates in the YSZ side. At a distance x away from oHp we denote the volumetric net charge density as $\rho_{(z)}$ and the Volta potential difference as

$$\Delta\Psi_{(z)} = \Psi_{(z)} - \Psi^{\mathrm{YSZ}} \quad , \qquad \text{(A1)}$$

where $\Psi_{(z)}$ and Ψ^{YSZ} are the Volta potential at position z and the bulk YSZ ($z \to \infty$), respectively. In this study the Volta potential of the bulk YSZ is set to zero. $\Delta\Psi_{(z)}$ is therefore reduced to $\Psi_{(z)}$. The relationship between $\rho_{(z)}$ and $\Psi_{(z)}$ is derived from the Gauss's law of electrostatics,

$$\begin{aligned} &\sum_{\mathrm{i}} \Phi_{\mathrm{i}} = \oiint_{\mathrm{S}} E_{\mathrm{G}}\,\mathrm{d}S = \frac{q_{\mathrm{enclosed}}}{\varepsilon_0\varepsilon_{\mathrm{r}}} \rightleftharpoons \Phi_{E_{\mathrm{G}},\text{face-left}} + \Phi_{E_{\mathrm{G}},\text{face-right}} + \Phi_{E_{\mathrm{G}},\text{side}} = \frac{\rho_{(z)}\mathrm{d}V}{\varepsilon_0\varepsilon_{\mathrm{r}}} \\ &\rightleftharpoons \pi r^2 E = \pi r^2 \left(-\frac{\mathrm{d}\Psi_{(z)}}{\mathrm{d}z} \right) = \frac{\int_l^{l+\Delta z} \rho_{(z)}\pi r^2 \mathrm{d}z}{\varepsilon_0\varepsilon_{\mathrm{r}}} \end{aligned} \quad , \qquad \text{(A2)}$$

where $\Phi_{E_{\mathrm{G}}}$ is the electric flux, S the surface area of the Gaussian pillbox, V the volume of the Gaussian pillbox, ε_0 the vacuum permittivity, ε_{r} the relative static permittivity of YSZ in the G–C layer, E the electric field in the G–C layer, and q_{enclosed} the electric charges enclosed by the Gaussian pillbox, *i.e.* the net electric charges at LSV side (with vanishingly small distance away from the LSV/YSZ interface) balanced with oxygen vacancies at oHp. In Eq. A2, $\Phi_{E_{\mathrm{G}}}$ consists of the electric flux of the left face ($\Phi_{E_{\mathrm{G}},\text{face-left}}$), the right face ($\Phi_{E_{\mathrm{G}},\text{face-right}}$) and the side ($\Phi_{E_{\mathrm{G}},\text{side}}$) of the Gaussian pillbox. Differentiating the last right hand of Eq. A2 against z leads to Poisson's equation,

$$\frac{\mathrm{d}^2\Psi}{\mathrm{d}z^2} = -\frac{\rho_{(z)}}{\varepsilon_{\mathrm{r}}\varepsilon_0} \quad . \qquad \text{(A3)}$$

In Eq. A3 and also in below, the subscript (z) is omitted merely for notational simplicity (*e.g.* $\Psi_{(z)}$ as Ψ). The relationship between ρ and Ψ lies in the defect chemistry of YSZ. The charged species in

YSZ are created by doping Y_2O_3 into ZrO_2 according to the overall reaction (using Kröger–Vink notations),

$$Y_2O_3 \xrightarrow{2\,ZrO_2} 2Y_{Zr}^{'} + V_O^{\bullet\bullet} + 3O_O^X \quad . \quad \text{(A4)}$$

$Y_{Zr}^{'}$ and $V_O^{\bullet\bullet}$ dominants according to the Assumption *v*. Under SOFC operating conditions ρ is then given by

$$\rho_{(z)} = e_0 \sum_i n_i z_i = e_0 \left(n_{Y_{Zr}^{'}} z_{Y_{Zr}^{'}} + n_{V_O^{\bullet\bullet}} z_{V_O^{\bullet\bullet}} \right) = e_0 \left(-n_{Y_{Zr}^{'}} + 2n_{V_O^{\bullet\bullet}} \right) , \quad \text{(A5)}$$

where $n_{Y_{Zr}^{'}}$ and $n_{V_O^{\bullet\bullet}}$ are the concentration of $Y_{Zr}^{'}$ and $V_O^{\bullet\bullet}$, respectively. Eq. A4 implies $n_{Y_{Zr}^{'}}$ and $n_{V_O^{\bullet\bullet}}$ fulfils

$$n_{Y_{Zr}^{'}}^0 = 2n_{V_O^{\bullet\bullet}}^0 , \quad \text{(A6)}$$

where $n_{Y_{Zr}^{'}}^0$ and $n_{V_O^{\bullet\bullet}}^0$ are the bulk concentration of $Y_{Zr}^{'}$ and $V_O^{\bullet\bullet}$, respectively. As the mobility of $Y_{Zr}^{'}$ is in orders of magnitude lower than that of $V_O^{\bullet\bullet}$ at elevated temperatures, $n_{Y_{Zr}^{'}}$ is assumed to remain constant (as $n_{Y_{Zr}^{'}}^0$) while $n_{V_O^{\bullet\bullet}}$ is potential-dependent and follows the Boltzmann distribution law. This behaviour of charged species in YSZ is distinct to that in aqueous solutions where both cations and anions are freely mobile. Charge concentrations of YSZ are then expressed as

$$n_{Y_{Zr}^{'}} = n_{Y_{Zr}^{'}}^0 , \quad \text{(A7–1)}$$

$$n_{V_O^{\bullet\bullet}} = n_{V_O^{\bullet\bullet}}^0 \exp\left(-\frac{U}{kT} \right) , \quad \text{(A7–2)}$$

where *U* is the potential energy, *k* the Boltzmann constant, and *T* the absolute temperature. Here *U* is negative because $V_O^{\bullet\bullet}$ are accumulated to balance the charge in the LSV. *U* simply becomes the

coulombic potential energy of $V_O^{\bullet\bullet}$ with the exclusion of short-range interactions (*e.g.* dispersion forces),

$$U = z_{V_O^{\bullet\bullet}} e_0 \Psi = 2e_0 \Psi \quad (\Psi < 0) . \quad \text{(A8)}$$

Incorporating Eqs. A3, A5, A6, A7, and A8 one gets

$$\frac{d^2\Psi}{dz^2} = \frac{2e_0 n_{V_O^{\bullet\bullet}}^0}{\varepsilon_r \varepsilon_0}\left[1 - \exp\left(-\frac{2e_0}{kT}\Psi\right)\right] , \qquad \text{(A9–1)}$$

or in another form

$$\frac{d^2\Psi}{dz^2} = -\frac{4e_0 n_{V_O^{\bullet\bullet}}^0}{\varepsilon_r \varepsilon_0}\sinh\left(\frac{e_0}{kT}\Psi\right)\exp\left(-\frac{e_0}{kT}\Psi\right) , \qquad \text{(A9–2)}$$

with the initial condition

$$\Psi_{z=z_{oHp}} = \Psi^{oHp} - \Psi^{YSZ} = \Psi^{oHp} , \quad \text{(A10–1)}$$

and the boundary conditions

$$\lim_{z \to z_{oHp}^+} \frac{d\Psi_G}{dz} = \lim_{z \to z_{oHp}^-} \frac{d\Psi_H}{dz} \qquad \text{(A10–2)}$$

and

$$\lim_{z \to \infty} \Psi = 0, \ \lim_{z \to \infty} \frac{d\Psi}{dz} = 0 . \quad \text{(A10–3)}$$

Eq. A9 has been the quintessential form that describes the spatial Volta potential variations of the G–C layer. It can be linearized if $2e_0\Psi$ is much smaller than kT (say, ten times), which is equivalent to a Ψ value not higher than 5 mV. Here the difficulty is that $\Psi_{(z)}$ is hard to be determined experimentally. To a rather qualitative guesstimate, Ψ is highly implausible of only several mV, taking typical OCV values (*ca* 1.2 V) under H_2 atmosphere into account. To conclude, Eq. A9 cannot be linearized under SOFC operating conditions. The boundary condition, Eq. A10–3, is provided only for an explanatory purpose. It is useless in solving Eq. A9, albeit useful to derive the differential capacitance (see below).

The following session is dedicated to derive the Gouy−Chapman capacitance (C_G) in function of the Volta potential. Recall the well-known relationship between E and Ψ

$$E = -\frac{d\Psi}{dz} \quad . \qquad \text{(A11)}$$

The $\Psi - E$ relationship is obtained by substituting Eq. A11 into Eq. A9–1,

$$E\frac{dE}{d\Psi} = \frac{2e_0 n^0_{V_O^{\cdot\cdot}}}{\varepsilon_r \varepsilon_0}\left[1 - \exp\left(-\frac{2e_0}{kT}\Psi\right)\right] . \qquad \text{(A12)}$$

One of the analytical solutions of Eq. A12 that is physically meaningful is

$$E = -\frac{d\Psi}{dz} = -\sqrt{\frac{2kTn^0_{V_O^{\cdot\cdot}}}{\varepsilon_r \varepsilon_0}\exp\left(-\frac{2e_0}{kT}\Psi\right) + \frac{4e_0 n^0_{V_O^{\cdot\cdot}}}{\varepsilon_r \varepsilon_0}\Psi + C} \quad , \qquad \text{(A13)}$$

where C is the constant to be determined. Applying Eq. A10–3 to Eq. A13 one gets

$$C = -\frac{2kTn^0_{V_O^{\cdot\cdot}}}{\varepsilon_r \varepsilon_0} \quad . \qquad \text{(A14)}$$

Substituting Eq. A14 back into Eq. A13 one yields

$$\left(\frac{d\Psi}{dz}\right) = \sqrt{\frac{2n^0_{V_O^{\cdot\cdot}}}{\varepsilon_r \varepsilon_0}}\sqrt{kT\left[\exp\left(-\frac{2e_0}{kT}\Psi\right) - 1\right] + 2e_0\Psi} \quad . \qquad \text{(A15)}$$

Eq. A15 cannot be solved analytically anymore. Fortunately Eq. A15 is quite enough to obtain C_G. According to the Gauss's law of electrostatics it reads

$$\sigma_G = \varepsilon_r \varepsilon_0 \left(\frac{d\Psi}{dz}\right)_{z=z_{oHp}} \quad , \qquad \text{(A16)}$$

where σ_G is the area specific charge density on the faces of Gaussian pillbox (Fig. 3a). Substituting Eq. A15 into Eq. A16 one obtains

$$\sigma_{\mathrm{G}} = \sqrt{2\varepsilon_{\mathrm{r}}\varepsilon_0 n^0_{\mathrm{V_O^{\cdot\cdot}}}}\sqrt{kT\left[\exp\left(-\frac{2e_0}{kT}\Psi_{\mathrm{G}}\right)-1\right]+2e_0\Psi_{\mathrm{G}}} \quad . \qquad \text{(A17)}$$

C_{G} is obtained by differentiating σ_{G} against Ψ,

$$C_{\mathrm{G}} = \frac{\mathrm{d}\sigma_{\mathrm{G}}}{\mathrm{d}\Psi_{\mathrm{G}}} \quad . \quad \text{(A18)}$$

Finally, one gets the relationship between C_{G} and Ψ_{G} by substituting Eq. A17 into Eq. A18,

$$C_{\mathrm{G}} = e_0\left[\exp\left(-\frac{2e_0}{kT}\Psi_{\mathrm{G}}\right)-1\right]\sqrt{\frac{2\varepsilon_{\mathrm{r}}\varepsilon_0 n^0_{\mathrm{V_O^{\cdot\cdot}}}}{kT\left[\exp\left(-\frac{2e_0}{kT}\Psi_{\mathrm{G}}\right)-1\right]+2e_0\Psi_{\mathrm{G}}}} \quad . \qquad \text{(A19)}$$

Appendix B: Relative static permittivity, ionic conductivity, diffusion coefficient, and free oxygen vacancy concentration of YSZ in the double layer regions and at elevated temperatures– a brief review

Relative static permittivity. The relative static permittivity (ε_r) of bulk YSZ at room temperature roughly falls in the range of 15 to 40.[2] Its high temperature values, however, have been poorly investigated. This rarity probably arises from the experimental difficulty, where the wicking and blistering of blocking electrodes (e.g., sputtered dense noble metal films) breaks down the ideal capacitive behaviour of electrochemical cells at elevated temperatures. Generally speaking, the ε_r measurement becomes unreliable if the temperature is higher than 600 °C. ε_r is thus not easily to be determined at 950 °C, the half-cell operating temperature adopted in this study. Steil et al. reported that $\varepsilon_r = 61$ at 350 °C, in contrast to $\varepsilon_r = 30$ at room temperature.[3] Perry and coworkers carefully measured a set of ε_r of lightly-sintered nano-crystalline YSZ samples at temperatures ranging from room temperature up to 410 °C. The $\varepsilon_r - T$ characteristic exhibited a sigmoid pattern that started to saturate *ca* 350 °C.[4] A bulk ε_r value of 77 at 950 °C was proposed in this study, by employing Steil's relative static permittivity data and Perry's temperature-dependent coefficient.

It is worth noting that ε_r falls dramatically near the double layer region. This phenomenon, known as "dielectric saturation", is attributed to dipole orientation and inductive atomic polarization effects. It had been well-studied in aqueous solutions that ε_r of water could drop from *ca* 78 (in the bulk) to 4 (in the innermost of the Helmholtz layer), depending on surface charge,[5] electric field,[6] ionic strength,[7] *etc*. Simulation works by means of Lorentz's local field theory indicated that ε_r can be reduced substantially in ultrathin film capacitors. The effect is fairly substantial for high ε_r materials (*e.g.* strontium-doped barium titanate) but relatively weak for low ε_r materials.[8] Similar effects had been somewhat observed in pulsed-laser deposited YSZ on Si wafer: ε_r were 19.8, 20.9, and 22.7, for film thicknesses of 9.0, 12.0, and 21.0 nm at room temperature, respectively.[9] However, it is still an open question on whether the thickness effect is still valid in the innermost double layer regions. More

relevant works has been carried out by Elshof and coworkers since 2001. They investigated the near-surface defect structures of YSZ in air and up to 577 °C.[10–12] Elshof et al. carefully discriminated the bulk ε_r values against the interfacial ε_r values. They also paid great attentions to temperature dependences of ε_r. While noticing that extrapolated ε_r values from low temperatures to high temperatures were too high to be physically realistic, they treated ε_r as a fitting parameter towards experimentally determined capacitance curves.[11] They recommended $\varepsilon_r = 14$ at 575 °C, by noting that all ε_r values fitted from capacitance–potential isotherms were within the range of 1 to 25.[12] These ε_r values are most likely to be interfacial ε_r values rather than bulk ε_r values. The bulk ε_r at 575 °C should be 68, if using the aforementioned arguments. Therefore, ε_r in the double layer regions is only of $\frac{1}{15}\sim\frac{1}{3}$ of the bulk ε_r value. Based on the above discussions, the relative static permittivity within the H–P layer and the G–C layer are assigned to be 10 and 24, respectively.

Ionic conductivity, diffusion coefficient, and free oxygen vacancy concentration. Oxygen vacancies of YSZ are created according to Eq. A4. The cubic fluorite structure of YSZ symbolizes 8 oxygen vacancies scattering randomly in 12.5 YSZ unit cells. The theoretical oxygen vacancy concentration ($n_{V_O^{\cdot\cdot}}^{th}$) is

$$n_{V_O^{\cdot\cdot}}^{th} = \frac{8}{12.5\,V_{cell}} = 0.\frac{64}{a^3} = 4.7\times10^{27}\,\frac{\square}{m^3}, \qquad \text{(B1)}$$

where V_{cell} is the volume of unit cell and a is the lattice parameter of YSZ. In reality, not all the oxygen vacancies are freely mobile even at elevated temperatures. A study on the activation enthalpy of ionic conductivity of single-crystalline 12 mol% yttria-stabilized zirconia indicated that oxygen vacancies were totally frozen below 400 °C and the ideal dissociation could never be achieved in foreseeable temperature region (>2000 °C).[13] To the best of our knowledge, such kinds of works, albeit relying on fragile and sensitive enthalpy data, had not been carried out in YSZ (caveat: YSZ in this work is for 8 mol% yttria-stabilized zirconia only). We utilize the Nernst–Einstein relationship, which

exists when the anion transport in solids is controlled by mobile anion vacancies, as an alternative approach to evaluate the free oxygen vacancy concentration ($n_{V_O^{\cdot\cdot}}$). The Nernst–Einstein equation for transport system under weak electrical fields can be written as[13]

$$\sigma_i = \frac{nq^2 D_s}{kT} \quad , \qquad \text{(B2)}$$

where n and q are the density and charge of freely mobile oxygen, respectively, D_s the oxygen self diffusion coefficient, and σ_i the ionic conductivity. Most reliable diffusion data are believed to be obtained from isotope exchange experiments. It is worth noting that it is the tracer diffusion coefficient (D_t), rather than D_s, that can be determined experimentally. D_s and D_t are connected by

$$D_t = f_D D_s \quad , \qquad \text{(B3)}$$

where f_D is the tracer correlation factor that accounts for the difference between actual vacancy jumps and effective vacancy jumps involving tracer ions.[14] An integral calculation suggested that for simple cubic lattice f_D is 0.6531 (caveat: oxygen diffusion in fluorite structure is actually in a generalized simple cubic structure).[15] σ_i in Eq. B2 is the ionic conductivity under small electric fields, but the electric field effect on σ_i is unlikely negligible. Thus, a correlation factor (f_c) should be introduced,

$$\sigma_i' = f_c \sigma_i \quad , \qquad \text{(B4)}$$

where σ_i' is the ionic conductivity determined experimentally. f_c of YSZ seems quiet pronounced. Manning et al. reported f_c at 550 °C, 700 °C, and 900 °C as 1.97, 0.59, and 1.35, respectively.[16] It exhibited positive temperature dependence at high temperatures (>700 °C) and vice versa.[16,17] The diffusive flux of oxygen must be compensated by a reverse flux of oxygen vacancies due to the elctroneutrality. $n_{V_O^{\cdot\cdot}}$, therefore, can be expressed as[16]

$$n_{V_O^{\cdot\cdot}}^0 = x_{V_O^{\cdot\cdot}}\left(1 - x_{V_O^{\cdot\cdot}}\right)n \approx x_{V_O^{\cdot\cdot}} n \quad , \text{(B5)}$$

where $x_{V_O^{\cdot\cdot}}$ is the fraction of oxygen lattice sites that are vacant, i.e., 8 %. $n^0_{V_O^{\cdot\cdot}}$ is expressed as experimentally measurable σ_i' and D_t by rearrangements of Eqs. B2, B3, B4, and B5,

$$n^0_{V_O^{\cdot\cdot}} = \frac{x_{V_O^{\cdot\cdot}} \sigma_i' kT f_D}{q^2 D_t f_c} \quad . \text{(B6)}$$

To evaluate the magnitude of $n^0_{V_O^{\cdot\cdot}}$ pragmatically, we only review some pertinent published results on the ionic conductivity and the tracer diffusivity of oxygen ions in YSZ but bypass underlying charge and mass transport mechanisms. σ_i' can be determined from four probe dc polarization cells with either Hebb-Wagner or van der Pauw configuration,[18] but the ac impedance technique had been more popular in solid electrolyte cells. In the way of D_t measurement, samples are usually annealed in designed O^{18}/O^{16} atmosphere for prolonged period. Concentration depth profiles are characterized via secondary ion mass spectroscopy (SIMS). They are subsequently fitted to the Fick's first law using D_t as a fitting parameter.

Figure S2 shows the reported conductivities [17,19–25] and the tracer diffusion coefficients[16,17,26–28] at elevated temperatures. The averaged value of σ_i at 950 °C is found to be 0.146 ± 0.016 S/cm. This value is interpolated from the conductivity data (Fig. S2) rather than from the Arrhenius plots, as the activation enthalpy is somewhat undefined in the Arrhenius plots. In contrast to the conductivity data, rare and inconsistent diffusivity data had been reported. Although Manning and coworkers' works seem to be more comprehensive than the others, we estimate a D_t value of 4×10^{-7} cm^2/s at 950 °C by means of interpolation. The free oxygen vacancy concentration $n^0_{V_O^{\cdot\cdot}}$ is then estimated to be about 1.4×10^{27} $/m^3$ (Eq. B6), almost one third of the upper limit given in Eq. B1.

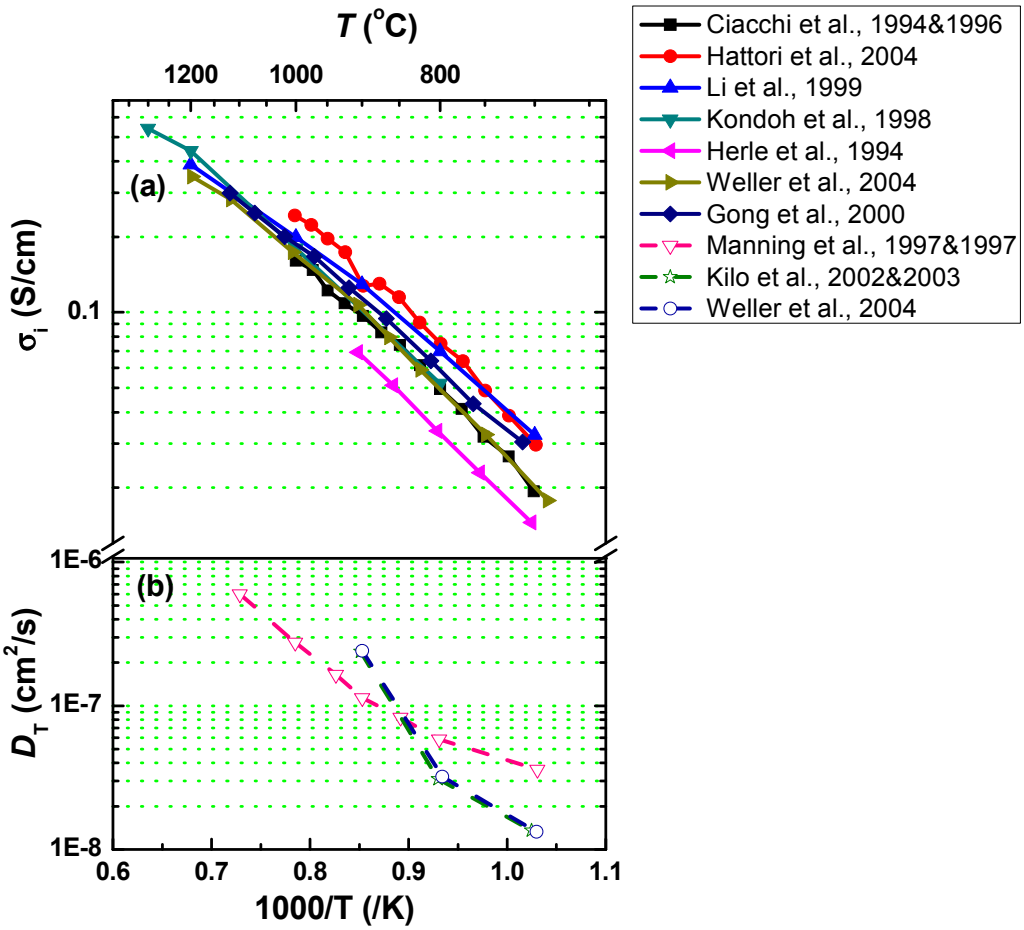

Figure S1. Arrhenius plots of (a) ionic conductivity (filled symbols) of YSZ, and (b) tracer diffusion coefficient (open symbols) of yttria-doped zirconia with various ytrria content (9.5 – 12 m/o) at elevated temperatures. Lines shown in the figure are merely guides for the eyes.

References:

1. (a) W. J. Duffin, *Electricity and Magnetism* (4th Ed.), McGraw-Hill, Maidenhead, 1990., pp. 82–90; W. M. Saslow, *Electricity, Magnetism, and Light*, Academic Press, Toronto, 2002, pp. 145–159.

2. (a) P. J. Harrop and J. N. Wanklyn, *Brit. J. Appl. Phys.*, 1967, **18**, 739.; (b) B. Cox, *Brit. J. Phys. D.*, 1968, **1**, 671.; (c) M. A. Subramanian and R. D. Shannon, *Mater. Res. Bull.*, 1989, **24**, 1477.; (d) M. T. Lanagan, J. K. Yamamoto and S. G. Sankar, *Mater. Lett.*, 1989, **7**, 437.; (e) K. C. Lau and B. I. Dunlap, *J. Phys.: Condens. Matter.* 2009, **21**, 145402.; (f) M. G. H. M. Hendriks, W. E. V. Zyl, J. E. T. Elshof and H. Verweij, *Mater. Res. Bull.*, 2001, **36**, 2395.

3. M. C. Steil, F. Thevenot and M. Kleitz, *J. Electrochem. Soc.*, 1997, **144**, 390.

4. N. H. Perry, S. Kim and T. O. Mason, *J. Mater. Sci.*, 2008, **43**, 4684.

5. D. Grahame, *J. Chem. Phys.*, 1950, **18**, 903.

6. B. E. Conway, J. O'M. Bockris and I. A. Ammar, *Trans. Faraday. Soc.*, 1951, **47**, 756.

7. R. G. Barradas and J. M. Sedlek, *Electrochim. Acta*, 1972, **17**, 683.

8. K. Natori, D. Otani and N. Sano, *Appl. Phys. Lett.*, 1998, **73**, 632.

9. S. J. Wang, C. K. Ong, S. Y. Xu, P. Chen, W. C. Tjiu, A. C. H. Huan, W. J. Yoo, J. S. Lim, W. Feng and W. K. Choi, *Semicond. Sci. Technol.*, 2001, **16**, L13.

10. J. E. T. Elshof, M. G. H. M. Hendriks, H. J. M. Bouwmeester and H. Verweij, *J. Mater. Chem.*, 2001, **11**, 2564.

11. M. G. H. M. Hendriks, J. E. T. Elshof, H. J. M. Bouwmeester and H.Verweij, *Solid State Ionics*, 2002, **146**, 211.

12. M. G. H. M. Hendriks, J. E. T. Elshof, H. J. M. Bouwmeester and H.Verweij, *Solid State Ionics*, 2002, **154-155**, 467.

13. J. D. Solier, I. Cachadiña, and A. Dominguez-Rodriguez, *Phys. Rev. B*, 1993, **48**, 3704.

14. K. Park and D. R. Olander, *J. Electrochem. Soc.*, 1991, **138**, 1154.

15. (a) G. L. Montet, *Phys. Rev. B*, 1973, **7**, 650.; (b) M. Helmut, *Diffusion in Solids: Fundamentals, Methods, Materials, Diffusion-Controlled Processes*, Chapter 7; Springer, Berlin Heidelberg, 2007.

16. P. S. Manning, J. D. Sirman, R. A. De Souza and J. A. Kilner, *Solid State Ionics*, 1997, **100**, 1.

17. M. Weller, R. Herzog, M. Kilo, G. Borchardt, S. Weber and S. Scherrer, *Solid State Ionics*, 2004, **175**, 409**.**

18. (a) I. Riess, *Solid State Ionics*, 1992, **51**, 219.; (b) Z. L. Zhang, X. E. Verykios and M. Baerns, *Catal. Rev.*, 1994, **36**, 507.; (c) P. Han and W. L Worrell, *J. Electrochem. Soc.*, 1995, **142**, 4235.; (d) I. Riess, *Solid State Ionics*, 1996, **91**, 221. ; (e) I. Riess, in *The CRC Handbook of Solid State Electrochemistry* (Edited by P. J. Gellings and H. J. M. Bouwmeester), Chapter 7; CRC Press, 1997.

19. F. T. Ciacchi, K. M. Crane, S. P. S. Badwal, *Solid State Ionics*, 1994, **73**, 49.

20. F. T. Ciacchi, S. A. Nightingale and S. P. S. Badwal, *Solid State Ionics*, 1996, **86-88**, 1167.

21. M. Hattori, Y. Takeda, Y. Sakaki, A. Nakanishi, S. Ohara, K. Mukai, J. H. Lee and T. Fukui, *J. Power Sources*, 2004, **126**, 23.

22. Y. Li, Z. L. Tang and Z. T. Zhang, *J. Mater. Sci. Lett.*, 1999, **18**, 443.

23. J. Kondoh, T. Kawashima, S. Kikuchi, Y. Tomii and Y. Ito, *J. Electrochem. Soc.*, 1998, **145**, 1527.

24. J. V. Herle, A. J. Mcevoy and K. R. Thampi, *J. Mater. Sci.*, 1994, **29**, 3691.

25. J. H. Gong, Y. Li, Z. L. Tang and Z. T. Zhang, *Mater. Lett.*, 2000, **46**, 115.

26. P. S. Manning, J. D. Sirman and J. A. Kilner, *Solid State Ionics*, 1997, **93**,125.

27. M. Kilo, C. Fundenberger, C. Argirusis, M. A. Taylor, G. Borchardt, M. Weller, R. A. Jackson, *Radiation Effects & Defects in Solids* , 2002, **157**, 1077.

28. M. Kilo, C. Argirusis, G. Borchardt and R. A. Jackson, *Phys. Chem. Chem. Phys.*, 2003, **5**, 2219.